



THE UNIVERSITY *of* EDINBURGH

Edinburgh Research Explorer

## Direct transmission detection of tunable mechanical resonance in an individual carbon nanofiber relay

**Citation for published version:**

Eriksson, A, Lee, S, Sourab, AA, Isacsson, A, Kaunisto, R, Kinaret, JM & Campbell, EEB 2008, 'Direct transmission detection of tunable mechanical resonance in an individual carbon nanofiber relay', Nano Letters, vol. 8, no. 4, pp. 1224-1228. <https://doi.org/10.1021/nl080345w>

**Digital Object Identifier (DOI):**

[10.1021/nl080345w](https://doi.org/10.1021/nl080345w)

**Link:**

[Link to publication record in Edinburgh Research Explorer](#)

**Document Version:**

Peer reviewed version

**Published In:**

Nano Letters

**Publisher Rights Statement:**

Copyright © 2008 by the American Chemical Society. All rights reserved.

**General rights**

Copyright for the publications made accessible via the Edinburgh Research Explorer is retained by the author(s) and / or other copyright owners and it is a condition of accessing these publications that users recognise and abide by the legal requirements associated with these rights.

**Take down policy**

The University of Edinburgh has made every reasonable effort to ensure that Edinburgh Research Explorer content complies with UK legislation. If you believe that the public display of this file breaches copyright please contact [openaccess@ed.ac.uk](mailto:openaccess@ed.ac.uk) providing details, and we will remove access to the work immediately and investigate your claim.



This document is the Accepted Manuscript version of a Published Work that appeared in final form in *Nano Letters*, copyright © American Chemical Society after peer review and technical editing by the publisher. To access the final edited and published work see <http://dx.doi.org/10.1021/nl080345w>

Cite as:

Eriksson, A., Lee, S., Sourab, A. A., Isacsson, A., Kaunisto, R., Kinaret, J. M., & Campbell, E. E. B. (2008). Direct transmission detection of tunable mechanical resonance in an individual carbon nanofiber relay. *Nano Letters*, 8(4), 1224-1228.

Manuscript received: 04/02/2008; Accepted: 21/02/2008; Article published: 06/03/2008

## Direct Transmission Detection of Tunable Mechanical Resonance in an Individual Carbon Nanofibre Relay\*\*

Anders Eriksson,<sup>1</sup> SangWook Lee,<sup>1,2</sup> Abdelrahim A. Sourab,<sup>1</sup> Andreas Isacsson,<sup>3</sup> Risto Kaunisto,<sup>4</sup>  
Jari M. Kinaret<sup>3</sup> and Eleanor E. B. Campbell<sup>1,5\*</sup>

<sup>[1]</sup>Department of Physics, Göteborg University, Göteborg, SE-412 96, Sweden.

<sup>[2]</sup>Department of Physics, Konkuk University, Seoul 143-701, Korea.

<sup>[3]</sup>Department of Applied Physics, Chalmers University of Technology, SE-412 96 Göteborg, Sweden.

<sup>[4]</sup>Nokia Research Center, P.O. Box 407, FIN-00045 Nokia Group, Helsinki, Finland.

<sup>[5]</sup>EaStCHEM, School of Chemistry, Joseph Black Building, University of Edinburgh, West Mains Road, Edinburgh, EH9 3JJ, UK.

<sup>[\*]</sup>Corresponding author; e-mail address: [Eleanor.Campbell@ed.ac.uk](mailto:Eleanor.Campbell@ed.ac.uk)

<sup>[\*\*]</sup>The authors are grateful for helpful discussions with A. Deleniv, P. Delsing, D. Dubuc, F. Kusidlo, P. Linnér, A. Masud, B. Starmark, M. Sveningsson, Y. Tarakanov, J. Wallinheimo and B. Witkamp. Financial support from the EU NANORF STREP programme, The Knut and Alice Wallenberg Foundation, the Swedish Strategic Research Foundation, the Korea Research Foundation Grant funded by the Korean Government (MOEHD) and Nokia Research Center is gratefully acknowledged. This paper reflects the views of the authors and not necessarily those of the EC. The community is not liable for any use that may be made of the information contained herein.

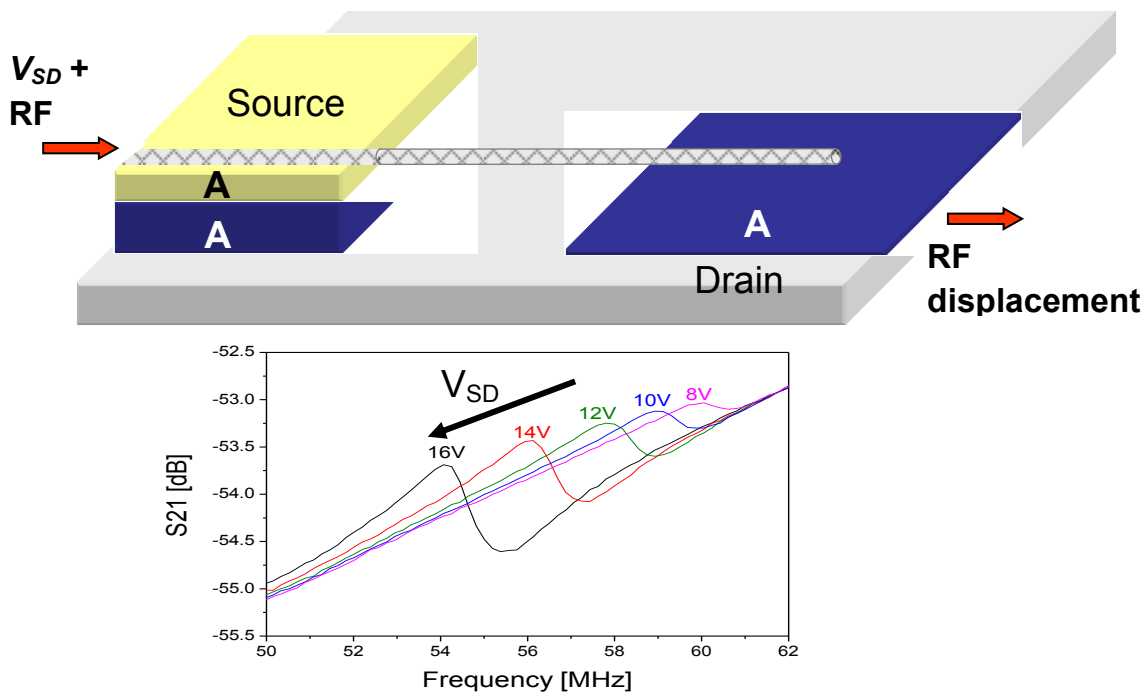
### Supporting information:

Measurement Circuit. This material is available free of charge via the Internet at <http://pubs.acs.org>

### Keywords:

Nanotubes; nanorelay; tunable RF transmission; nems

## Graphical abstract



## Abstract

A direct on-chip transmission measurement of the resonance frequency of an individual singly-clamped carbon nanofibre relay is reported. The experimental results are in good agreement with a small signal model and show the expected tuning of the resonance frequency with changing bias voltage.

## Introduction

Nanoelectromechanical systems (NEMS) are attracting increasing attention due to their small size, low power consumption and fast switching speeds<sup>[1]</sup>. They are regarded as among the most interesting emerging technologies on the ITRS road map<sup>[2]</sup>. Carbon nanotubes are particularly interesting as NEMS components due to their low mobile mass and high Young's modulus, which enables high speed, combined with their high mechanical strength and ability to withstand extreme conditions of temperature and radiation exposure. The predicted possibility of tuning the resonance frequency over a large range by the application of a gate voltage<sup>[3]</sup> is particularly promising for many

applications. Here we present a direct transmission measurement of the resonance frequency of an individual singly-clamped carbon nanofibre relay. The experimental results verify the predictions of a small signal model and provide important information for determining the practicality of using carbon-based NEMS as components in real electrical circuits.

Some prototype carbon NEMS have been reported in the literature <sup>[4-11]</sup> but there have been relatively few experimental studies of the high frequency properties of carbon NEMS based on individual carbon nanotubes <sup>[12-16]</sup>. The resonance frequencies of doubly clamped suspended single-walled nanotubes (SWNT) have been determined using an indirect mixing technique with a lock-in amplifier <sup>[12-14]</sup>. The method requires a semiconducting nanotube and can therefore not be applied to the mechanically more rigid multi-walled nanotubes (MWNT) or nanofibres (CNF) that have been studied as DC prototype NEMS and allow the fabrication of more varied device geometries <sup>[4-8, 10, 11]</sup>. The mechanical resonances of singly-clamped MWNT have been observed in a field emission microscope where the broadening of the field emission spot was observed as the nanotube was brought into mechanical resonance by the application of an AC voltage on a side gate. The resonance frequency of the MWNT could be tuned by an order of magnitude by increasing the bias voltage on the nanotube and thus increasing the tension <sup>[15]</sup>. The same technique has recently been used to demonstrate a so-called nanoradio <sup>[16]</sup>. Although all of these studies provide interesting information concerning the resonance properties of individual carbon nanotubes, they do not provide much needed information on the feasibility of integrating carbon-based NEMS in useful electronic circuits nor on the signal levels that can be expected. In this letter we report the first direct transmission detection of the resonant behaviour of a two-terminal carbon nanofibre relay. We compare the experimental data with the predictions of a small signal model, treating the CNF as a simple series resonator. Good agreement is obtained concerning the resonance amplitude, shape and phase. We show that it is possible to measure the transmission of a single relay device; however, the signal level is very low and most practical applications will need to be based on arrays of such structures.

A schematic diagram of the device is shown in Fig. 1 along with the substrate layout and equivalent circuit model. The small signal model is expected to be valid if the bias voltage applied between the source and the drain electrode,  $V_{SD}$ , is much greater than the amplitude of the AC voltage applied in series at the source electrode,  $V_{AC}$ , i.e. in the regime of linear response. When a DC bias voltage is applied, the CNF becomes charged with respect to the drain electrode and a capacitive coupling is induced. If the CNF is at mechanical resonance the electric field will vary harmonically thus inducing a surface current at the drain electrode that can be detected.

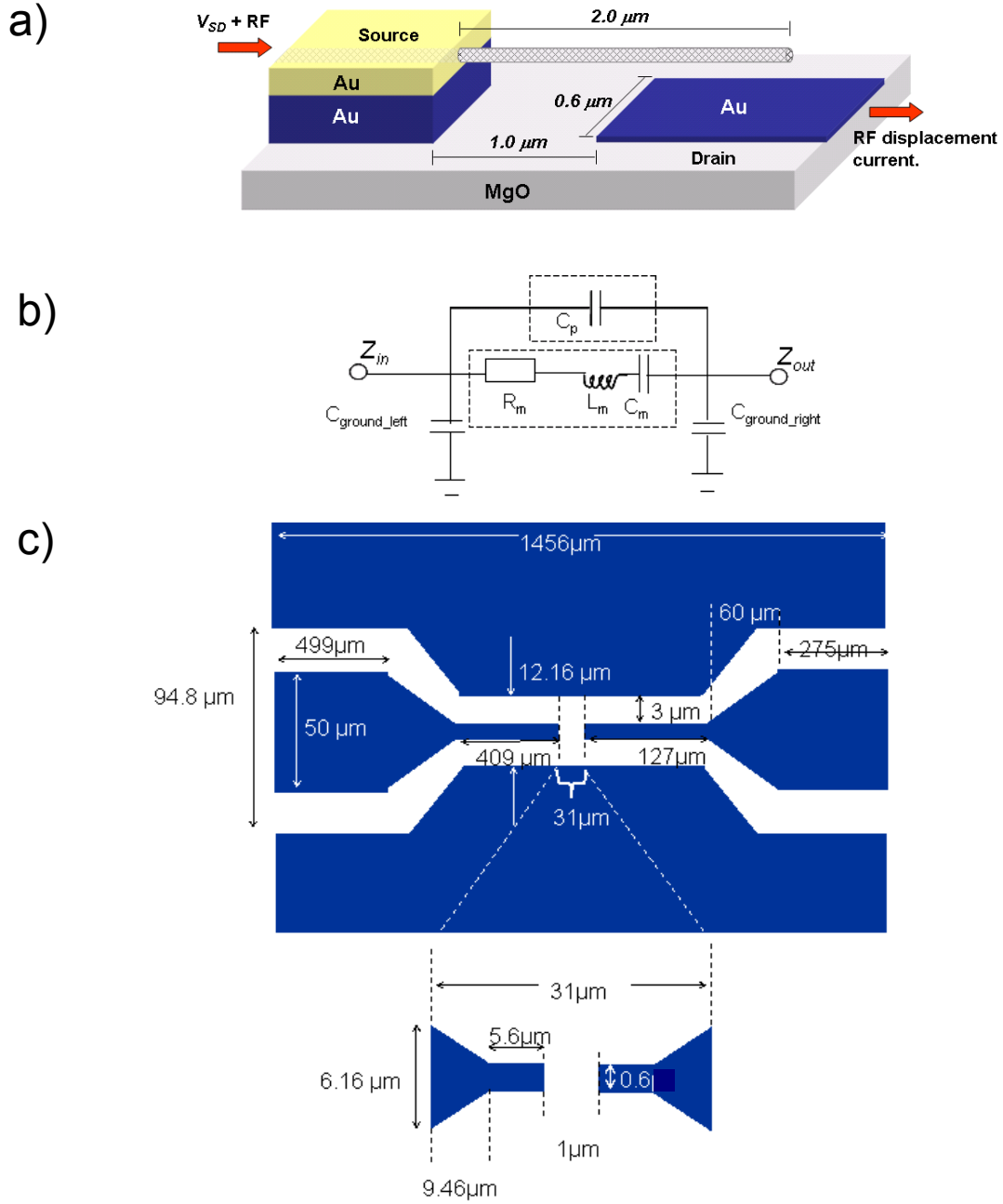


**Figure 1.** (a) Schematic drawing of two-terminal CNF relay. (b) Equivalent circuit (c) Substrate layout, designed to reduce parasitic capacitance. Note, drawing is not to scale.

The equivalent motional parameters for the resonator, Fig. 1(b), are given by <sup>[17]</sup>:

$$L_m = \frac{m_{eff}}{V_{SD}^2 \cdot C_D'(x)} ; C_m = \frac{1}{L_m \cdot \omega^2} ; R_m = \frac{\omega_0}{Q_0} L_m + R_C , \quad [1]$$

where  $m_{eff} \approx m/5.687$  is the effective mass of the CNF ( $m$  is its physical mass),  $V_{SD}$  is the DC bias voltage,  $\omega_0$  and  $\omega$  are the intrinsic and tuned resonant frequencies of the CNF,  $Q_0$  is the intrinsic mechanical/frictional Q-factor of the resonator and  $R_C$  is the contact resistance between the resonator and the source electrode. The derivative of the capacitance at the quiescent point,  $C'_D(x)$ , is given by:

$$C'_D(x) = \frac{C_{D0} \Delta_{CNF-Drain}}{(\Delta_{CNF-Drain} - x)^2}, \quad [2]$$

where  $\Delta_{CNF-Drain}$  is the static unbiased equilibrium distance between the suspended CNF and the drain electrode,  $x$  is the static down-deflection of the CNF for a given DC bias,  $V_{SD}$ , and  $C_{D0}$  is the static unbiased equilibrium capacitance between the CNF and the drain electrode<sup>[18]</sup>. The motional inductance and capacitance are thus determined theoretically by the geometry of the device, the Young's modulus of the CNF and the applied bias voltage,  $V_{SD}$ . The motional resistance is then set by the intrinsic Q-factor,  $Q_0$ , and the contact resistance,  $R_C$

$$\frac{1}{Q_L} = \frac{1}{Q_{R_m}} + \frac{1}{Q_{R_L}} = \frac{\omega_0}{\omega \cdot Q_0} + \frac{R_C}{\omega \cdot L_m} + \frac{Z_{in} + Z_{out}}{\omega \cdot L_m} \quad [3]$$

where  $Z_{in}$  and  $Z_{out}$  are the input and output impedance, respectively (Fig. 1(b),  $Z_{in} = 50 \Omega$ ,  $Z_{out} = 100 \Omega$ ). The expression is dominated by the first term.

A magnesium oxide single crystal wafer (Tateho Chemical Industries Co. Ltd.) was chosen as substrate. MgO has a similar dielectric constant (9.65 at 1 MHz) to alumina (9.6 at 1 MHz) which is normally used as a substrate for RF measurements and is also employed in standard SOLT ('short', 'open', 'load', 'thru') calibration substrates. The smooth epi-polished surface of the MgO proved to be more suitable for nanoscale electrode fabrication than the commercially available alumina substrates. The micron scale coplanar waveguide and ground plate region were patterned by photolithography whereas the nanometer scale source and drain electrodes were patterned in between the coplanar lines using e-beam lithography. The source electrode was patterned to have its surface lying 220 nm above that of the drain electrode (note however, that the suspended nanostructure may not be exactly horizontal and the distance of the tip to the drain electrode may be less than the electrode height difference). The relay device is prepared by depositing dispersed carbon nanofibres using AC dielectrophoresis. The method has been described previously<sup>[19]</sup> and was used to fabricate prototype three-terminal nanorelays<sup>[4]</sup>. Due to the highly insulating nature of the substrate, it is not possible to image the device using electron microscopy. For this reason, we have had to use relatively large (50-100 nm diameter, 2-3  $\mu\text{m}$  long) carbon nanofibres prepared by DC plasma-enhanced chemical vapour deposition<sup>[20]</sup>. These structures are just large enough to be imaged with a good optical microscope which allows us to check for the presence and alignment of the carbon

nanostructure before the RF measurements. Although these nanostructures are mainly hollow (typically with bamboo-like partitioning), they do not have the highly crystalline structure of good quality multi-walled nanotubes and we prefer to refer to them as nanofibres to clarify this distinction. Arrays of carbon nanofibres are grown on a Si wafer and then removed and dispersed in sodium dodecyl sulfate (SDS) before being deposited on the source electrode in the presence of a 16V peak-to-peak AC voltage at a frequency of 13MHz. After all fabrication steps have been completed, the device is checked in an optical microscope and then mounted on a printed circuit board containing an operational amplifier circuit. S-parameter measurements were performed using an Agilent ENA Network-Analyzer (E7501B). Calibration was done using a SOLT CS-5 calibration substrate and GSG ('ground'-'signal'-'ground') probes with 200  $\mu\text{m}$  pitch were employed for all measurements. All experiments were done under high vacuum conditions ( $5 \times 10^{-8}$  Torr) at room temperature. After measurement, the device geometry was checked in a scanning electron microscope after the evaporation of a 25 nm thick gold film to avoid charging problems.

The substrate layout, Fig. 1(c), has been designed to minimize parasitic cross-talk, making it feasible to realize a broad-band detection scheme using transmission detection with a standard network analyzer. A similar approach was followed by Husain et al. for measurements on a platinum nanowire resonator<sup>[21]</sup>. The simulated (MOMENTUM ADS) and measured parasitic thru-capacitances for our substrate were found to be 350 aF and 230 aF respectively. Even with an optimized substrate design, the output levels expected from the small signal model were below parasitic contributions. An operational amplifier circuit was connected to the output of the NEMS resonator to provide a gain of 50dB. The details of the final circuit design and measurement setup are supplied in the Supplementary Information.

The resonance signal from a nanofibre relay is shown in Fig. 2 as a function of the source-drain voltage,  $V_{SD}$ . The tunability of the resonance peak can be clearly seen. The frequency shift shows the expected  $V_{SD}^2$  dependence up to relatively high bias voltages ( $>15$  V), Fig. 2(c). Beyond this, the measured frequency appears to saturate and in some cases, even increases (see data points at 18V in Fig. 2(b)). There are two possible reasons for such behaviour. The first is the "guitar" effect<sup>[15]</sup> where the electrostatic force induces tension in the CNF that increases the resonance frequency. The second possibility is that the CNF has come into contact with impurity particles present at the source electrode thereby effectively shortening its suspended length and increasing the resonant frequency. Although we can be sure that we have a large nanofibre resonator in place before the measurements, we cannot completely rule out the presence of much smaller structures at the source electrode that can also be deposited during the nanofibre deposition step. SEM images of the devices after operation indicate the presence of such structures. The data in Fig. 2 (c) indicate the likelihood of the second

explanation since the reverse scan frequencies are simply shifted slightly upwards in frequency but show the same slope as for the forward scan.

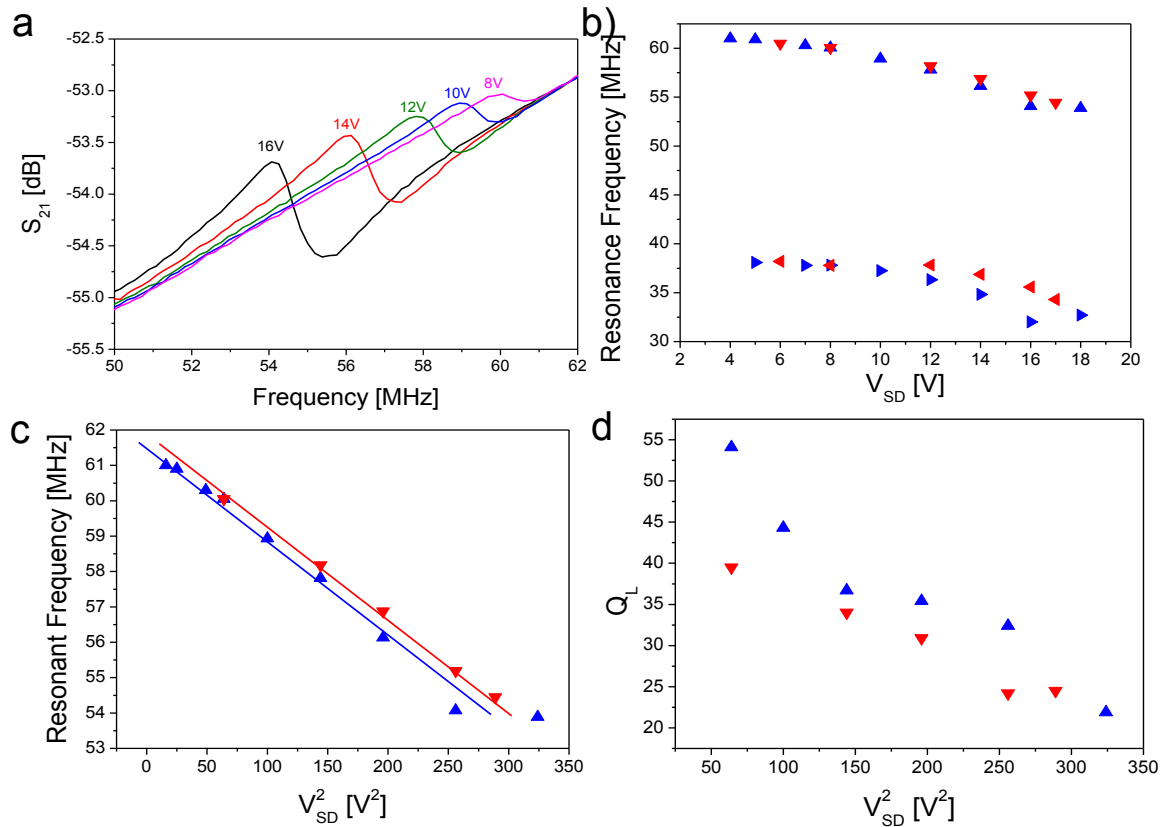


**Figure 2.** (a) Transmission signal,  $S_{21}$  parameter, for a two-terminal CNF relay. The resonance frequency is tuned downwards as the source-drain voltage,  $V_{SD}$ , is increased. (b) Resonance frequency versus  $V_{SD}$  for two resonators. Blue symbols, forward voltage scan. Red symbols, reverse voltage scan. (c) Resonant frequency vs  $V_{SD}^2$  for the higher of the two resonances shown in (b). The frequency shift is linear with  $V_{SD}^2$  as expected from the small signal model. The departure from linear behaviour at high voltages and the slight shift upwards in frequency on the reverse scan is attributed to geometrical changes occurring on the first voltage scan. (d) The loaded Q-factor,  $Q_L$ , obtained from the fitted motional impedance parameters for the high frequency resonator.

Experimentally, the motional impedance parameters are extracted from the measurements by simulating the entire system in the ADS circuit simulator where the operational amplifier circuit was represented by a SPICE model and the series resonator was embedded in circuit parameters measured for the coplanar layout on the MgO substrate. The fit to the small signal model is very good

confirming that the device can be modeled as a series resonator. Examples of the fit to the transmission signal and the phase are shown in Fig. 3 for the higher frequency device at a source-drain voltage of 17 V yielding  $R_m = 82 \text{ M}\Omega$ ,  $C_m = 1.45 \text{ aF}$  and  $L_m = 5.7 \text{ H}$ .

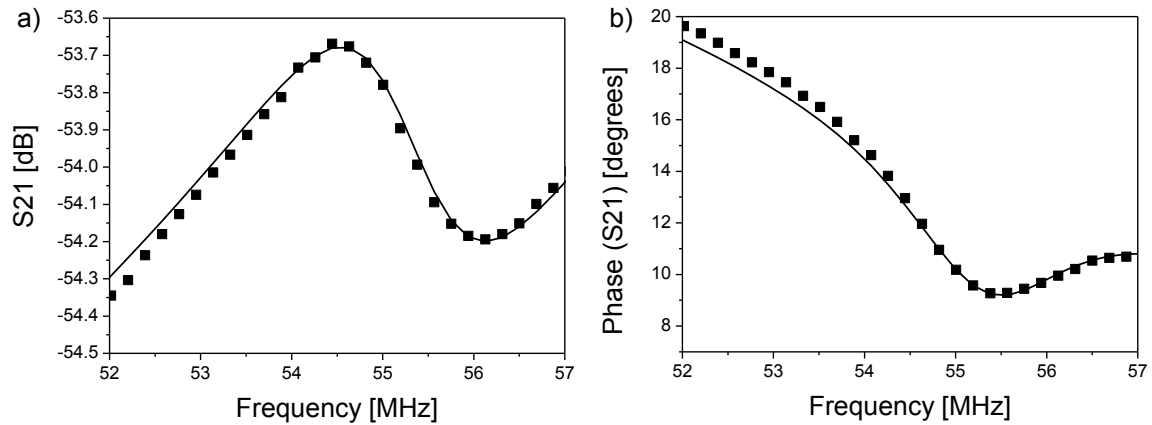


**Figure 3.** (a) Amplitude  $S_{21}$  and (b) phase for the high frequency resonance with  $V_{SD} = 17\text{V}$ . The experimental data is shown as square symbols. The full lines are obtained from assuming small signal model behaviour and simulating the entire system in the ADS circuit simulator. By fitting the model to the experimental data it is possible to extract the motional impedance parameters,  $R_m$ ,  $C_m$  and  $L_m$ .

The loaded Q-factors that were extracted from the fitted motional impedance parameters are quite low, ranging from  $Q_L = 54$  for  $V_{SD} = 8\text{V}$  to  $Q_L = 22$  at  $V_{SD} = 18\text{V}$ , Fig. 2(d). The highest Q-factors we have measured are on the order of 200. However, a more reproducible and better controlled fabrication procedure, yielding cleaner devices, will be necessary to significantly improve the operation. The qualitative trend in  $Q_L$  is also as expected, Fig. 2(d) but again there appears to be evidence of a change in device behaviour as the source-drain voltage is increased on the first scan.

The results of a quantitative comparison between the theoretical and experimental small signal model parameters are illustrated in Fig. 4. Here we have chosen to compare the experimental data up to  $V_{SD} = 16\text{V}$ , covering the upwards voltage sweep range where the resonance frequency shifts with  $V_{SD}^2$ , as expected. The dimensions of the resonator were estimated from SEM pictures, taken after the device was coated with a thin gold film to avoid charging, CNF length =  $2.05 \mu\text{m}$ , CNF diameter =  $100 \text{ nm}$ , giving an effective mass of  $3.4 \text{ fg}$ , and initial height above drain electrode =  $120 \text{ nm}$ . The theoretical model has three adjustable parameters; the Young's modulus of the CNF,  $C_{D0}$  and  $Q_0$ . The comparison is shown for a Young's modulus of  $0.41 \text{ TPa}$ ,  $C_{D0} = 4.5 \text{ aF}$  and  $Q_0 = 47$ . The fitted

Young's modulus is within the expected range for CNF. The quantitative agreement is very good for the resonant frequency and  $R_m$  dependence. The agreement between the measured and calculated  $C_m$  and  $L_m$  shows slightly more scatter but is still quite good.

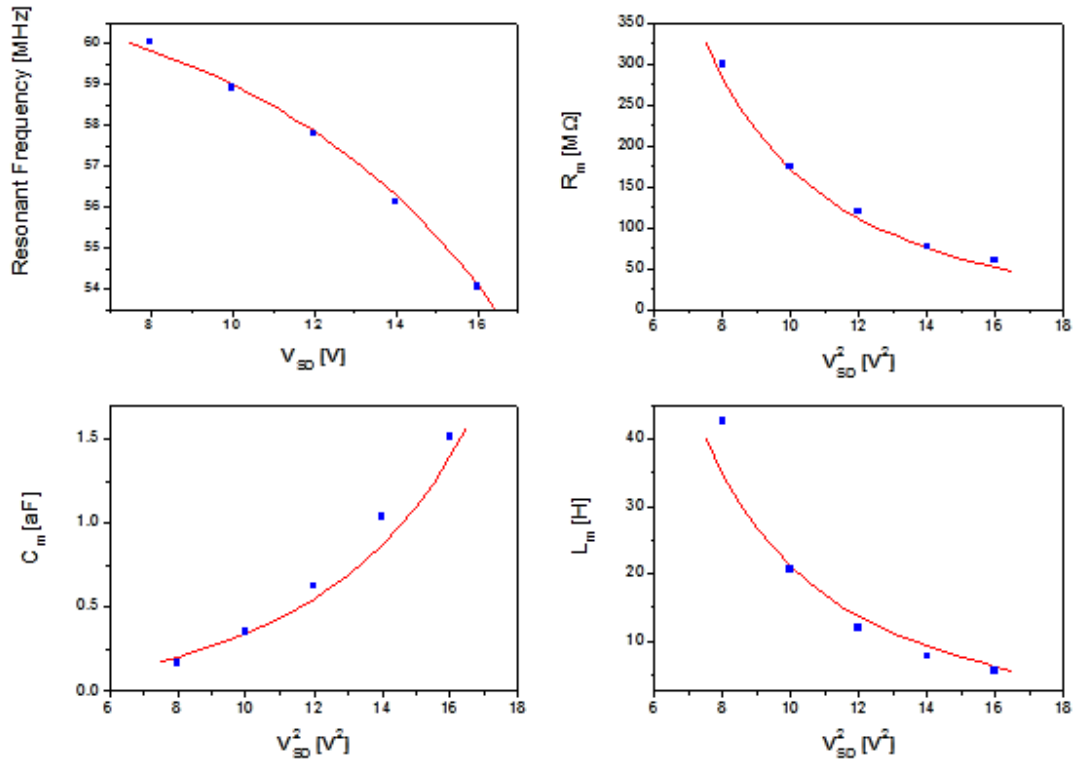


**Figure 4.** Comparison of the small signal nanotube resonator model to the experimental results. The device geometry was estimated from SEM images. Squares (blue) are measurements and the red lines are theoretical predictions obtained with CNF Young's modulus  $E=0.41$  TPa,  $C_{D0}=4.5$  aF and  $Q_0=47$ .

We have demonstrated the first direct transmission measurements on individual, singly-clamped CNF resonators using a broadband capacitive coupling technique and shown the tuning of the resonant frequency with the applied source-drain DC voltage. The results are in good agreement with a small signal model and provide valuable input for evaluating the usefulness of carbon nanotube and nanofibre NEMS for applications in electronics. The method should be applicable to smaller MWNT devices with appropriate changes to the amplifier circuit to move the broadband detection window to higher frequencies. The difficulty resides with observing the device before measurement, essential if a deposition fabrication technique is used. The problem could be overcome if the nanotube device could be reliably grown in the desired position with the desired geometry. Work towards this goal is in progress.

## References

- [1] Cleland, A. N. *Foundations of Nanomechanics*; (Springer-Verlag: Berlin, 2003).
- [2] <http://www.itrs.net/reports.html>
- [3] Jonsson, L.M., Axelsson, S., Nord, T., Viefers, S., Kinaret, J.M., High frequency properties of a CNT-based nanorelay, *Nanotechnology* 15, 1497-1502 (2004)
- [4] Lee, S.W., Lee, D.S., Morjan, R.E., Jhang, S.H., Sveningsson, M., Nerushev, O.A., Park, Y.W., Campbell, E.E.B., A three-terminal carbon nanorelay, *Nano Lett.* 4, 2027-2030 (2004)
- [5] Dujardin, E., Derycke, V., Goffman, M.F., Lefèvre, Bourgoin, J.P., Self-assembled switches based on electroactuated multiwalled nanotubes, *Appl. Phys. Lett.* 87, 193107 (2005)
- [6] Jang, J.E., Cha, S.N., Choi, Y.J., Kang, D.J., Butler, T.P., Hasko, D.G., Jung, J.E., Kim, J.M., Amaratunga, G.A.J., Nanoscale memory cell based on a nanoelectromechanical switched capacitor, *Nature Nanotechnology* 3, 26-30 (2008)
- [7] Kim, P., Lieber, C.M., Nanotube nanotweezer, *Science* 286, 2148- (1999)
- [8] Kaul, A.B., Wong, E.W., Epp, L., Hunt, B.D., Electromechanical carbon nanotube switches for high-frequency applications, *Nano Lett.* 6, 942-947 (2006)
- [9] Rueckes, T., Kim, K., Joselevich, E., Tseng, G.Y., Cheung, C.-L., Lieber, C.M., Carbon nanotube-based non-volatile random access memory for molecular computing, *Science*, 289, 94-97 (2000)
- [10] Fennimore, A.M., Yuzvinsky, T.D., Han, W.O., Fuhrer, M.S., Cumings, J., Zettl, A., Rotational actuators based on carbon nanotubes, *Nature* 424, 408-410 (2003)
- [11] Cohen-Karni, T., Segev, L., Srur-Lavi, O., Cohen, S.R., Joselevich, E., Torsional electromechanical quantum oscillations in carbon nanotubes, *Nature Nanotechnology* 1, 36-41 (2006)
- [12] Sazanova, V., Yaish, Y., Ustinel, H., Roundy, D., Arias, T.A., McEuen, P.L., A tunable carbon nanotube electromechanical oscillator, *Nature* 431, 284-287 (2003)
- [13] Witkamp, B., Poot, M., van der Zant, H.S.J., Bending-mode vibration of a suspended nanotube resonator, *Nano Lett.* 6, 2904-2908 (2006)
- [14] Peng, H.B., Chang, C.W., Aloni, S., Yuzvinsky, T.D., Zettl, A., Ultrahigh frequency nanotube resonators, *Phys. Rev. Lett.* 97, 087203 (2006)

- [15] Purcell, S.T., Vincent, P., Journet, C., Binh, V.T., Tuning of nanotube mechanical resonances by electric field pulling, *Phys. Rev. Lett.* 89, 276103 (2002)
- [16] Jensen, K., Weldon, J., Garcia, H., Zettl, A., Nanotube radio, *Nano Lett.* 7, 3508-3511 (2007)
- [17] Truitt, P.A., Hertzberg, J.B., Huang, C.C., Ekinici, K.L., Schwab, K.C., Efficient and sensitive capacitive readout of nanomechanical resonator arrays, *Nano Lett.* 7, 120-126 (2007)
- [18] Isacsson, A., Kinaret, J.M., Kaunisto, R., Nonlinear resonance in a three-terminal carbon nanotube resonator, *Nanotechnology* 18, 195203 (2007)
- [19] Lee, S.W., Lee, D.S., Yu, H.Y., Campbell, E.E.B., Park, Y.W., *Appl. Phys. A* 78, 283-286 (2004)
- [20] Morjan, R.E., Kabir, M.S., Lee, S.W., Nerushev, O.A., Lundgren, P., Bengtsson, S., Park, Y.W., Campbell, E.E.B., Selective growth of individual multiwalled carbon nanotubes, *Current Appl. Phys.* 4, 591-594 (2004)
- [21] Husain, A., Hone, J., Postma, H.W.C., Huang, X.M.H., Drake, T., Barbic, M., Scherer, A., Roukes, M.L., Nanowire-based very-high-frequency electromechanical resonator, *Appl. Phys. Lett.* 83 1240-1242 (2003).